HHS Public Access

Author manuscript

Chem Res Toxicol. Author manuscript; available in PMC 2024 July 21.

Published in final edited form as:

Chem Res Toxicol. 2024 July 15; 37(7): 1218–1228. doi:10.1021/acs.chemrestox.4c00149.

Mass Spectrometric Detection and Differentiation of Enzymatically Active Abrin and Ricin Combined with a Novel Affinity Enrichment Technique

Suzanne R. Kalb,

National Center for Environmental Health, Division of Laboratory Sciences, Centers for Disease Control and Prevention, Atlanta, Georgia 30341, United States

Kaitlyn K. Drinkard,

National Center for Environmental Health, Division of Laboratory Sciences, Centers for Disease Control and Prevention, Atlanta, Georgia 30341, United States

John R. Barr

National Center for Environmental Health, Division of Laboratory Sciences, Centers for Disease Control and Prevention, Atlanta, Georgia 30341, United States

Abstract

Abrin and ricin are toxic proteins produced by plants. Both proteins are composed of two subunits, an A-chain and a B-chain. The A-chain is responsible for the enzymatic activity, which causes toxicity. The B-chain binds to glycoproteins on the cell surface to direct the A-chain to its target. Both toxins depurinate 28S rRNA, making it impossible to differentiate these toxins based on only their enzymatic activity. We developed an analytical workflow for both ricin and abrin using a single method and sample. We have developed a novel affinity enrichment technique based on the ability of the B-chain to bind a glycoprotein, asialofetuin. After the toxin is extracted with asialofetuin-coated magnetic beads, an RNA substrate is added. Then, depurination is detected by a benchtop matrix-assisted laser desorption/ionization time-of-flight (MALDI TOF) mass spectrometer to determine the presence or absence of an active toxin. Next, the beads are subjected to tryptic digest. Toxin fingerprinting is done on a benchtop MALDI-TOF MS. We validated the assay through sensitivity and specificity studies and determined the limit of detection for each toxin as nanogram level for enzymatic activity and μg level for toxin fingerprinting. We examined potential cross-reactivity from proteins that are near neighbors of the toxins and examined potential false results in the presence of white powders.

Corresponding Author: Suzanne R. Kalb – National Center for Environmental Health, Division of Laboratory Sciences, Centers for Disease Control and Prevention, Atlanta, Georgia 30341, United States; skalb@cdc.gov.

Author Contributions

K.K.D.: data curation, methodology, investigation, writing—original draft. S.R.K. Conceptualization, data analysis, supervision, project administration, writing—review and editing. John R. Barr: conceptualization, funding acquisition, supervision, writing—review and editing. CRediT: **Kaitlyn K. Drinkard** conceptualization, data curation, formal analysis, investigation, validation, writing-original draft; **John Robert Barr** funding acquisition, project administration, supervision, writing-review & editing; **Suzanne Ramirez Kalb** conceptualization, formal analysis, funding acquisition, project administration, supervision, writing-review & editing.

The authors declare no competing financial interest.

Complete contact information is available at: https://pubs.acs.org/10.1021/acs.chemrestox.4c00149

INTRODUCTION

Ricin and abrin toxins are type II ribosome-inactivating protein toxins (RIP-II toxins) and are classified as select agents by the CDC due to their accessibility and potential for bioterrorism.[1] Both toxins are extracted from commonly available plant products. Ricin is extracted from the seeds of the plant *Ricinus communis*. The seeds are used to make castor oil. Castor oil has a number of medicinal, pharmaceutical, and industrial uses ranging from a laxative and drug delivery vehicle to biodiesels, soaps, greases, fertilizers, and paints.[2,3] Abrin is extracted from seeds of the plant *Abrus precatorius*, commonly known as rosary peas. Rosary peas are popularly used in jewelry around the world.[4] Although rosary peas are not in as high demand as castor seeds, the toxin extracted from rosary peas is reported to be more toxic than ricin., with an LD_{50} of 0.01–0.04 μg/kg for abrin compared to 0.1–1 μg/kg for ricin.[4] In their pure form, both toxins exist as white powders and are stable over wide pH and temperature ranges. Both toxins can be fatal from ingestion, inhalation, and injection. This increases their potential for use as bioterror weapons.

RIP-II toxins are glycoprotein-binding lectins. They are composed of two subunits that are approximately equal in size and that are connected by a disulfide bond. The B-chain binds to terminal galactoses on glycoproteins on cell membranes.[5–7] Specifically, ricin is reported to bind to β-1,4-galactoses and *N*-acetylgalactosamine carbohydrates.[5] The A-chain enters the cell and depurinates 28S rRNA, causing cell death.[4] Both subunits must be present in vivo for the toxin to have an effect. Because the toxins have two subunits, it is necessary for detection methods to observe both the presence of the B-chain and the enzymatic activity of the A-chain to provide a more complete understanding of the potential threat of the sample.[8]

Several strategies have been adopted to detect ricin or abrin, including direct detection of the toxins,[9] detection of the RIP activity,[10] and detection of DNA from plants that make the toxins to infer the presence of toxin.[11] Typically, analytical methods have focused on assays that can detect ricin or abrin, but not both toxins, in the same analysis. Methods that directly detect ricin or abrin include immunological assays such as enzyme-linked immunosorbent assays (ELISA),[12–16] lateral flow immunochromatography,[12,17,18] and mass spectrometry-based methods.[19] Most mass-spectrometry-based methods[19] and some immunological assays can differentiate ricin from the closely related *R. communis* agglutinin (RCA120)[20] and abrin from *A. precatorius* agglutinin.[21,22] There are a few methods that can directly detect and differentiate ricin and abrin in a single assay.[23–25] There are also some methods that detect ricin or abrin RIP activity, including cell-based assays[26,27] and depurination of an RNA or DNA substrate that mimics the natural rRNA substrate of RIP.[19,28–30] Cell-based assays are limited because components of complex matrices can trigger cell death, while depurination assays only measure one aspect of the toxicity, and neither type of assay can differentiate ricin from abrin. Additionally, polymerase chain reaction (PCR) assays and immunocapture methods, such as ELISA and lateral flow, only prove the presence of the toxin. They do not distinguish between active and inactive toxins or measure the ability of the toxin to bind to the cell membrane. These measurements are needed to assess the public health threats associated with these toxins.

Previously, our laboratory described a ricin detection workflow that uses antibody-coated magnetic beads to detect enzymatic activity, followed by a tryptic digest to confirm the structure of the toxin.[28] While this method addresses both toxin activity and confirmation of toxin structure, it is limited to ricin and does not report the ability of the toxin B-chain to bind glycoproteins. In the case of a release of these toxins, it would be critical for public health laboratories to be able to determine the presence of these toxins to mitigate the effects on people exposed and effectively decontaminate exposed areas. Additionally, these mass spectrometric methods used sensitive, but sophisticated instrumentation that may not be readily available for public health laboratories. Another method for ricin detection uses more accessible benchtop MALDI-TOF mass spectrometers and galactose-bound amine beads instead of antibody-coated streptavidin beads.[31] These beads can detect activity and confirm structure but are limited to ricin only.

Because ricin and abrin have similar mechanisms of action and cause similar symptoms, an assay that could detect and differentiate between both would be beneficial for public safety. Furthermore, an assay that measures both A-chain enzymatic activity and the ability of the B-chain to bind galactose on cell membrane[32–35] glycoproteins would give a more comprehensive idea of the biological threat. Both of these attributes would allow public health laboratories to efficiently test for both toxins to gain a more complete understanding of the threat. In this article, we describe a method that uses glycoprotein to extract both ricin and abrin, measures the depurination activity of both, and differentiates toxins by the detection of tryptic fragments on a benchtop MALDI TOF mass spectrometer.

MATERIALS AND METHODS

Safety Statement.

Due to their toxicity, experimentation with ricin and abrin requires enhanced safety measures. All work with toxins was performed in certified level 2 biological safety cabinets equipped with HEPA filters in a select agent-registered laboratory.

Materials.

Ricin, its individual chains, and RCA120 were obtained from Vector Laboratories. Abrin was purchased from Toxin Technologies. Streptavidin Dynabeads were purchased from Invitrogen. EZ-link Sulfo-NHS-Biotin was purchased from Thermo Fisher Scientific. Trypsin (gold, mass spectrometry grade) was purchased from Promega. All chemicals were purchased from Sigma-Aldrich unless noted otherwise. RNA14A substrate (rCrGrCrGrCrGArGrArGrCrGrCrG) was synthesized by Integrated DNA Technologies (IDT). MBT Biotarget 96 disposable plates were purchased from Bruker Daltonics Inc. Our near neighbors (protein toxins with similar enzymatic activity) were prepared according to previous specifications.[36] Instant dry milk was purchased from a local grocery store. White powder stock solutions were prepared at 1 mg/mL in water. Kinetics buffer and consumables for the Octet R8 were purchased from Sartorius. Amicon Ultra 0.5 Centrifugal 3 kDa molecular weight cutoff filters were used to remove excess biotin in kinetics studies. Aldehyde and amine-terminated magnetic beads were purchased from BioClone Inc.

Bead Coupling.

Amine-terminated magnetic beads were prepared by washing 1 mL of beads with 5 mL of 10 mM pyridine, pH 6 (coupling buffer). The washed beads were suspended in 5 mL of 5% glutaraldehyde and placed on a gentle rotation for 1 h. After 1 h, beads were washed 3 times with coupling buffer. Glycans (as listed in Table 1) were coupled to beads by combining 1 mL of 2 mg/mL glycan dissolved in coupling buffer and placing it on gentle rotation overnight. After coupling, beads were washed 3 times with 1 mL of phosphate-buffered saline (PBS) with TWEEN 20 (PBST). Then, the washed beads were suspended in 1 mL of 1× PBST.

Aldehyde-terminated magnetic beads were prepared using a coupling buffer of 0.1 M sodium phosphate, pH 7.0, a blocking buffer of 1 M Tris HCl, pH 7.4, a washing buffer of 1 M NaCl, and sodium cyanoborohydride (5 M dissolved in 1 M NaOH). Thirty mg of magnetic beads were weighed into a microcentrifuge tube. One mL of coupling buffer was used to resuspend beads. Coupling buffer supernatant was removed by retaining beads using a magnet; 1 mL of coupling buffer was added again. This was repeated twice to wash the beads. To couple the ligands, 0.5–10 mg of individual carbohydrates listed in Table 1 were dissolved in 1 mL coupling buffer and added to the beads. Then, 10 μL of sodium cyanoborohydride was added. Solution with the beads were placed on a rotisserie overnight at room temperature. After overnight incubation, beads were washed 3× with coupling buffer. Then, 1 mL of blocking buffer and 10 μL of sodium cyanoborohydride were added, and the beads were then incubated for 1 h at room temperature or for 4 °C overnight. Beads were then washed 4–6 times with 1 mL of washing buffer. Beads were resuspended in 1 mL of 1× PBST.

Streptavidin magnetic beads were coupled to glycoproteins by first biotinylating the glycoprotein (listed in Table 1). 16 μg/mL of asialofetuin was incubated with 0.267 mM biotin for 1 h at room temperature. Different concentrations of asialofetuin, from 10 to 160 mg/mL, were tested with incubation times of 1 h and overnight to find these optimized conditions. After biotinylation, 1 mL of streptavidin beads was washed with 1 mL of 1× PBST 3 times. The biotinylated protein solution was added to the beads and gently rotated for 1 h at room temperature. After rotation, beads were washed 3 times with 1× PBST and resuspended in 1× PBST.

Extraction of Toxins.

A Kingfisher with a magnetic tip comb was used to bind ligand-bound beads to the toxin by keeping beads and toxin in solution with constant agitation. One mL of sample consisting of 40 μL of beads; 1× PBST; and varying concentrations of abrin, ricin, ricin A-chain, or ricin B-chain was gently agitated for 1 h. After agitation, toxin-bound beads were washed with 1× PBST or 2 M NaCl followed by 1× PBST. The toxin-bound beads were then eluted into deionized water and transferred to PCR strip tubes. Beads were retained using a magnet, while water was removed from PCR strip tubes.

Activity Assay with MS Analysis.

Ammonium citrate (18 μL of 5 mM stock solution) with 1 mM ethylenediamineetraacetic acid, pH 4.1 (reaction buffer), was added to PCR strip tubes with 2 μL of 1 mM RNA-14A substrate (rCrGrCrGrCrGArGrArGrCrGrCrG) and vortexed gently to mix. The solution was incubated at 45 °C for 4 h. After incubation, magnetic beads were retained in PCR strip tubes using a magnet. Two μL of reaction supernatant was removed and added to 18 μL of 3-hydroxypocolinic acid (3-HPA) MALDI matrix (735 mM 3-hydropicolinic acid, 40 mM ammonium citrate, and 0.1% trifluoroacetic acid (TFA) in 50/50 acetonitrile/deionized water). It was vortexed gently to mix. Two μL of the matrix-sample mixture was spotted on an MBT Biotarget disposable 96-well plate, left to dry, and then spotted with 2 μL a second time. Next, they were run on a Bruker Microflex benchtop MALDI. Spots were analyzed from 1000 to 6000 m/z using positive ion linear mode. Spectra were processed by using Bruker FlexAnalysis software. The software identified the substrate mass of the intact RNA substrate as 4525 m/z and the depurinated product mass as 4408 m/z.

Multiple variations of this assay were performed. For white powders, 1 mL of a 1 mg/mL white powder solution was added to a sample well. The toxin level was 5× the limit of detection (LOD) for each toxin. To discourage inhibition of toxin by dry milk, 500 μL of lactase at 2 mg/mL was mixed with 500 μL of 1 mg/mL of all white powder solutions and incubated at 27 °C for 30 min before the toxin was spiked into the sample. Near neighbors were also tested, as previously described.[31]

Digestion with Trypsin and MS Analysis of Tryptic Fragments.

Toxin-bound beads were retained in PCR strip tubes by using a magnet. The supernatant was removed, and the beads were reconstituted in 16 μL of tryptic digest buffer (50 μM ammonium bicarbonate), 2 μL of 0.5 mg/mL trypsin, and 2 μL of acetonitrile. Samples were gently vortexed to mix and incubated at 62 °C for 30 min. This was followed by an incubation at 95 °C for 10 min to inactivate the toxin. After incubation, beads were retained with a magnet while 2 μL of reaction supernatant was added to 18 μL of α-cyano-4-hydroxycinnamic acid (CHCA) MALDI matrix (5 mg/mL CHCA, 1 M ammonium citrate, and 0.1% TFA in 50/50 solution of acetonitrile and deionized water). Two μL of sample-matrix mixture were spotted on a MBT biotarget disposable 96-well plate. Samples were analyzed from 800 to 6000 m/z using positive ion linear mode on the Bruker Microflex benchtop MALDI. FlexAnalysis software was used to process spectra and identify tryptic fragment peaks.

B-Chain Binding Assessment with Biolayer Interferometry.

Asialofetuin was biotinylated by incubating with a 20-fold molar excess of Sulfo-NHS Biotin at room temperature for 1 h. Excess biotin was removed by using a 3K molecular weight cutoff filter. The filters were prepared by adding 500 μL of 1× PBS solution and spinning in a microcentrifuge at 14,000 RCF for 10 min. The filtrate and retentate were discarded, and the biotinylated asialofetuin was added to the filters. The filters were spun at 14,000 RCF for 20 min. Next, the filtrate was discarded and the retentate was rinsed with 1X PBS and spun for 20 min at 14,000 RCF. Then, the retentate, containing the biotinylated asialofetuin, was collected.

Kinetic measurements were taken using streptavidin-coated sensors for the Sartorius Octet R8. The sensors were prewet with 1× kinetics buffer while the sample plate was prepared. A sensor check was performed for 60 s in 1× kinetics buffer. The sensors were then loaded with biotinylated asialofetuin at 1.5 μg/mL for 300 s. After loading, a baseline measurement was taken in 1× kinetics buffer for 60 s. Then, to measure association, the loaded sensors were introduced to the ricin B-chain at 10, 5, 2.5, 1.25, 0.63, and 0.31 μg/mL for 300 s. Control measurements were taken with the loaded sensors in a well-containing no ricin B-chain and with an unloaded sensor in a well-containing 10 μg/mL ricin B-chain. Then, disassociation was measured by removing the sensors from the ricin B-chain sample and introducing them to a well containing only 1× kinetics buffer for 600 s. Results were processed using the Octet Analysis software to fit curves for association and disassociation using a 1:1 binding model with a global fit.

RESULTS AND DISCUSSION

The goal of this work was to enhance preparedness by developing an analytical workflow that analyzes both ricin and abrin in a single sample. The workflow includes an activity assay to mimic the biological activity of the toxin and peptide fingerprinting to identify and differentiate the RIP toxins, as depicted in Figure 1. The benchtop MALDI TOF used in this study is available in many public health laboratories. To provide a better assessment of the toxin's activity, an affinity capture was developed to determine the B-chain's ability to bind to galactose. The depurination reaction on an RNA substrate shows the enzymatic activity of the A-chain.

Extraction of Ricin and Abrin with Simple Carbohydrate-Coated Beads.

Our laboratory previously optimized an RNA substrate (rCrGrCrGrCrGArGrArGrCrGrCrG; RNA14A) to detect ricin's enzymatic activity.[29] Although abrin and ricin are known to have the same enzymatic activity, it was not known if abrin would be able to depurinate this RNA substrate. In addition, a ricin detection method developed in our laboratory extracted ricin with 4-aminophenyl-1-thiol-β-D-galactopyranoside (APTG)-coated magnetic beads prior to depurination of the RNA substrate.[31] Because abrin also binds to glycans with terminal galactose,[7] we first attempted to adapt our previous ricin method to extract abrin. The 4-APTG beads, under the same conditions as those for extracting ricin, failed to extract abrin (data not shown).

Next, we prepared a variety of beads coated with various glycans, as listed in Table 1. Most of the combinations did not appear to extract abrin except for 4-aminoethyl-β-D-lactopyranoside (4-APLP) beads. The 4-APLP beads were able to extract abrin. The abrin was able to depurinate the synthetic RNA substrate, which was demonstrated by the loss of adenine from the RNA14A substrate. This resulted in a mass shift from m/z 4525 for the unmodified substrate to m/z 4408 in the MALDI TOF spectrum, corresponding to the toxin-mediated loss of adenine from the substrate (Figure 2). The LOD of the MALDI TOF depurination assay using 4-APLP beads to extract toxins was determined by testing abrin levels from 200 to 8 ng as shown in Figure 2. Depurination was not apparent at levels under 40 ng of abrin.

The 4-APLP beads were tested for their ability to extract ricin. Results showed complete depurination of the RNA14A substrate with 1 μg of ricin (data not shown), meaning that these beads were successful at extracting ricin and abrin. Although the 4-APLP beads were able to extract both toxins, the APLP-coated beads are expensive and labor intensive to make. They used several different buffers that need to be adjusted for pH and multiple reagents. Furthermore, the detection limits for abrin (40 ng/mL) were higher than we desired.

We then turned to glycoproteins instead of simple carbohydrates to better mimic the in vivo binding of the toxins because the B-chain is known to bind to glycoproteins with terminal galactose on the cell surfaces, and other laboratories have shown success with using glycoproteins to bind to ricin.[34,35] Ovalbumin, fetuin, asialofetuin, and α1-acid glycoprotein (Table 1) were biotinylated and tested as ligands coupled to streptavidin beads for their ability to pull down abrin. We measured the extraction of the toxins by observing the level of depurination of the RNA14A substrate. All glycoproteins tested, except ovalbumin, resulted in depurination of the RNA14A substrate. The failure of ovalbumin to extract abrin is likely due to the characteristics of the glycoprotein. There is only one *N*-glycosylation site in ovalbumin (ASN-292) and although terminal galactose-containing hybrid structures have been reported on ovalbumin, the glycans are dominated by high-mannose type glycans.[37,38] Samples extracted with asialofetuin showed the highest level of depurination, which is consistent with reports from studies by Wu et al. which reported the binding properties of these glycoproteins to abrin as asialofetuin > glycoproteins that contain sialyated glycans.[39] Asialofetuin extraction also showed a good depurination of the substrate with ricin. The asialofetuin-coated streptavidin beads had better performance and lower cost, and the bead preparation was simpler than the other glycoprotein streptavidin beads and the 4-APLP amine beads.

Asialofetuin Beads Binding to Toxin.

An advantage of using a glycoprotein-bound bead to extract the toxin is that the affinity capture is more general for RIP, better mimics the in vivo binding of these toxins, and diverse RIP can be differentiated with peptide mapping on a mass spectrometer. Because an intact toxin that has an A-chain and B-chain is required for in vivo toxicity and the depurination of the substrate is only attributed to the presence of the A-chain, we performed a series of experiments to show the binding and depurination properties of each chain alone when compared to the whole ricin toxin. The activity of the individual subunits with RNA14A substrate was compared when bound and unbound to asialofetuin beads. Unbound, 200 ng/mL of ricin A-chain shows activity through complete depurination of the substrate while the same amount of ricin B-chain shows no enzymatic activity (data not shown). This confirms that both individual chains of ricin are performing as expected. However, no depurination is seen for 200 ng/mL of the individual A-chain or the B-chain with the asialofetuin-beads extraction procedure (data not shown). The lack of depurination from the B-chain after the asialofetuin-bead extraction step can be explained because the B-chain does not have enzymatic depurination activity. After the asialofetuin extraction procedure, the A-chain sample did not show any depurination of the RNA substrate because it was not extracted by the beads. The combination of these results shows that asialofetuin beads are

binding to the B-chain of the toxin, allowing the A-chain to depurinate once the beads are introduced to the substrate. Thus, extraction of the toxins with glycoproteins coupled with the depurination reactions assesses the presence of both chains.

To characterize the binding of the B-chain to the asialofetuin beads, we used the Sartorius Octet R8 to measure the binding kinetics of the ricin B-chain to asialofetuin beads. The Sartorius streptavidin-coated biosensors allowed us to design an experiment that would closely resemble the toxin pull-down method we use for extracting toxins for activity analysis. After measuring the association and disassociation of ricin B-chain to asialofetuin, the Octet Analysis software was able to fit the kinetics curves using a 1:1 model with a global fit type. The software determined the K_D to be 1.935×10^{-8} M or 0.19 nM with an R^2 value of 0.9813 (Figure 3.)

The K_D measurement in the nanomolar range is considered high affinity and indicates that the asialofetuin is a good binding ligand for the ricin-B chain.[40,41] This combined with the lack of depurination seen from the ricin A-chain by extraction confirms that a positive enzymatic activity result is due to the presence of both toxin subunits. In this case, the B-chain is responsible for glycoprotein bead binding, and the A-chain is responsible for depurination of the RNA14A substrate.

Optimization of Asialofetuin Beads.

Toxin extraction with asialofetuin beads was optimized. Factors varied and tested include the ratio of biotin to asialofetuin, the length of time of biotinylation of asialofetuin, the ratio of asialofetuin to streptavidin beads, and the volume of asialofetuin-beads used to extract ricin and abrin. Asialofetuin bead production was determined to be most efficient for extracting toxin with 2.84 μg of biotin coupled to 16 μg of asialofetuin for 1 h and bound to 1 mL of streptavidin beads (data not shown). 40 μL of these beads was found to yield the best results with extraction for tryptic digestion, while 20 μL of beads was sufficient for activity. 40 μL of beads ensured both activity and structure portions of the assay were optimized, and we determined it was best for toxin extraction from samples.

Limit of Detection—Activity.

We defined the parameters for the LOD by comparing the intensity of the depurinated peak of the sample to the blank. It is not uncommon to see slight depurination of the substrate in a blank sample. Following an analysis of 60 blank runs, we found the most useful representation of depurination to be described by the ratio of signal-to-noise (SN). By comparing the ratio of the SN of the intact substrate (SN_i) to the depurinated substrate (SN_d), we can have a numerical representation of the difference in intensities. The differences reflect what we saw in the mass spectra. Our analysis of 60 blank runs yielded an average ratio of 0.0087 with a standard deviation of 0.0194. For a sample to be considered positive, the SN_d/SN_i needed to be three times this blank ratio.

For each toxin, a range-finding study was performed to determine the best levels for further investigation. This range consisted of 6, 8, 10, and 12 ng for abrin and 0.4, 0.5, 0.6, 0.8, and 1 ng for ricin. The results from the range-finding study indicated that more appropriate

levels were needed for both abrin and ricin. The ranges were expanded to also include 2 and 4 ng for abrin and 0.50, 0.75, 1, and 1.25 ng for ricin.

After a window was narrowed, several levels were tested over 20 runs. The SN_d/SN_i was calculated for each sample and compared to the average of the SN_d/SN_i of the blanks. Samples were considered positive if the SN_d/SN_i was three times that of the average SN_d/SN_i of the blanks. Using these defined criteria, the LOD was determined to be the lowest concentration that had a 95% positivity rate. For abrin, this was 4 ng (Table 2) and for ricin, it was 0.75 ng (Table 3).

Limit of Detection—Tryptic Digest.

Tryptic digests were performed for each toxin at three concentration levels over 20 runs. Ricin produced the most consistent tryptic fragments at 2 μg, and abrin at 20 μg. For both ricin and abrin, several fragments were frequently observed that are unique to *R. Communis* or *A. Precatorius* as shown in Table 4.

For a sample to be positive for ricin or abrin, the activity assay must be positive at greater than 3 times the blank, and a minimum of three toxin fragments must be detected in the MALDI TOF spectrum. We are aware that the low sensitivity of these instruments, when compared to more sophisticated mass spectrometers, is a hindrance to consistent tryptic fragment detection. We plan to develop a method that uses more sensitive instrumentation to aid public health laboratories when a reliable tryptic digest spectrum is difficult to obtain.

Differentiating Toxins.

A blind study was conducted to test the possibility of distinguishing ricin from abrin in this assay. Samples were prepared with no toxin, 2 μg/mL of toxin, and 20 μg/mL of toxin for both ricin and abrin. Activity and tryptic digest data were collected. The sample containing no toxin was easily identified with the activity assay, as it was the only negative sample (data not shown). All spiked samples showed positive activity and complete depurination of the RNA14A substrate (data not shown). Tryptic digest fragments were then compared to distinguish between ricin and abrin. Although very similar in structure, the tryptic fragments seen by MALDI for each toxin are mostly unique, as shown in Figure 4.

The similarities between spectra can be assumed to come from the partial digestion of asialofetuin-coated beads or trypsin itself. The blind samples were correctly identified as ricin or abrin.

Near Neighbors.

Other RIP toxins are known, and some have the same enzymatic activity as abrin and ricin. We collected extracts from a variety of near-neighbor plants and tested them to ensure that none would produce a false positive result. There were four extracts tested that had a positive activity result: *Cinnamomum camphora*, *Sambucus nigra*, *A. precatorius*, and *R. communis* as shown in Table 5.

A. precatorius and *R. communis* produce abrin and ricin, respectively, so this result was expected. Both *C. camphora* and *S. nigra* have RIP II toxins with the same enzymatic

activity as ricin and abrin and were extracted with asialofetuin beads. The RIP II lectins from *C. camphora* (cinnamomin 1, cinnamomin 2, cinnamomin 3, and cinphorin) and *S. nigra* (SNA-V, SNA-Vf, Nigrin l1, Nigrin l2, Nigrin s. SNA-I, SNA-I′, SNA-If, SNAflu-I, SNARP1, and SNLRP2)[42] bind to GalNAc residues. Bovine fetuin is known to have O-linked glycans that contain GalNAc.[43] When the extracts from *C. camphora*, *S. nigra* were tested for structural confirmation, all were negative. This distinguishes them from both abrin and ricin, with no false-positive results.

White Powders.

In the solid form, both toxins appear as a white powder. Common household white powders were tested in samples with and without each toxin to determine the possible interference with the beads. These results would help if the common powders are used to camouflage the toxins or if a white powder would give a false-positive result. All unspiked white powders gave a true-negative result (data not shown) Initially, all spiked samples, except for dry milk, showed positive activity (data not shown). Lactose is a strong binder to these RIP toxins; therefore, lactase was added to this sample to inhibit the binding, allowing the beads to bind to the toxin as normal. Adding lactase to all of the samples before bead binding, including the dry milk sample, yielded a positive activity result as shown in Table 6. Additionally, all spiked and unspiked white powders were tested by using the structure portion of the assay. In all cases, the unspiked white powders gave a negative result and all spiked white powders gave a positive result as shown in Table 6. Collectively, these experiments demonstrate the ability of this assay to distinguish abrin and ricin from white powders that are similar in appearance.

CONCLUSIONS

In the case of a bioterrorism event, the response time is critical. This entire assay is performed on a simple benchtop MALDI TOF, making it accessible for public health laboratories. The results are obtained in less than 1 day, can detect and distinguish between two RIP toxins of bioterrorism interest, and provide a complete picture of toxicity. Using a glycoprotein to mimic the in vivo activity of the toxin allows the assay to simultaneously detect the presence of the B-chain subunit of these toxins, which, while not necessary for enzymatic activity, is required for in vivo toxicity.

Several combinations of sugars, glycoproteins, and magnetic beads were tested for their ability to extract abrin toxin from samples and confirm its structure by tryptic digest. After several combinations with abrin were tested, the glycoprotein asialofetuin proved to be the most effective ligand when biotinylated and coupled to streptavidin beads. The glycoprotein ligand made the assay effective in analyzing a single sample for ricin and abrin in a single assay. Validation of the assay involved examination of the LOD and potential interferences. Abrin and ricin activities are detectable at 4 and 0.75 ng, respectively. Structural confirmation can be accomplished at toxin levels of 20 μg for abrin and 2 μg for ricin. This method can be adapted for more sophisticated equipment that could lower the limits of detection.

The presence of white powders did not interfere with these two portions of the assay if appropriate measures were taken. Specifically, if the toxin sample was suspected of containing white powders, then adding lactase before bead binding. Any possible false positives for the activity assay can be negated by tryptic digestion and structure analysis if similar toxins or near neighbors are present. In short, this assay fills a critical gap in detecting and differentiating the RIP toxins abrin and ricin.

ACKNOWLEDGMENTS

The findings and conclusions in this study are those of the authors and do not necessarily represent the official position of the U.S. Department of Health and Human Services, or the U.S. Centers for Disease Control and Prevention. Use of trade names and commercial sources is for identification only and does not constitute endorsement by the U.S. Department of Health and Human Services, or the U.S. Centers for Disease Control and Prevention.

REFERENCES

(1). Centers for Disease Control and Prevention, U. S. D. o. A. Select Agent and Toxins List. https://www.selectagents.gov/sat/list.htm (accessed on March 22, 2024).

(2). Patel VR; Dumancas GG; Viswanath LCK; Maples R; Subong BJJ Castor Oil: Properties, Uses, and Optimization of Processing Parameters in Commercial Production. Lipid Insights 2016, 9, 1–12. [PubMed: 27656091]

(3). Bradberry SM; Dickers KJ; Rice P; Griffiths GD; Vale JA Ricin poisoning. Toxicol. Rev 2003, 22 (1), 65–70. [PubMed: 14579548]

(4). Janik E; Ceremuga M; Saluk-Bijak J; Bijak M Biological Toxins as the Potential Tools for Bioterrorism. Int. J. Mol. Sci 2019, 20 (5), 1181. [PubMed: 30857127]

(5). Taubenschmid J; Stadlmann J; Jost M; Klokk TI; Rillahan CD; Leibbrandt A; Mechtler K; Paulson JC; Jude J; Zuber J; et al. A vital sugar code for ricin toxicity. Cell Res. 2017, 27 (11), 1351–1364. [PubMed: 28925387]

(6). Lin JY; Lee TC; Hu ST; Tung TC Isolation of four isotoxic proteins and one agglutinin from jequiriti bean (Abrus precatorius). Toxicon 1981, 19 (1), 41–51. [PubMed: 7222088]

(7). Bagaria A; Surendranath K; Ramagopal UA; Ramakumar S; Karande AA Structure-function analysis and insights into the reduced toxicity of Abrus precatorius agglutinin I in relation to abrin. J. Biol. Chem 2006, 281 (45), 34465–34474. [PubMed: 16772301]

(8). Bozza WP; Tolleson WH; Rivera Rosado LA; Zhang B Ricin detection: tracking active toxin. Biotechnol. Adv 2015, 33 (1), 117–123. [PubMed: 25481398]

(9). Despeyroux D; Walker N; Pearce M; Fisher M; McDonnell M; Bailey SC; Griffiths GD; Watts P Characterization of ricin heterogeneity by electrospray mass spectrometry, capillary electrophoresis, and resonant mirror. Anal. Biochem 2000, 279 (1), 23–36. [PubMed: 10683227]

(10). Pelham HR; Jackson RJ An efficient mRNA-dependent translation system from reticulocyte lysates. Eur. J. Biochem 1976, 67 (1), 247–256. [PubMed: 823012]

(11). Felder E; Mossbrugger I; Lange M; Wölfel R Simultaneous detection of ricin and abrin DNA by real-time PCR (qPCR). Toxins 2012, 4 (9), 633–642. [PubMed: 23105972]

(12). Xu C; Li X; Liu G; Xu C; Xia C; Wu L; Zhang H; Yang W Development of ELISA and Colloidal Gold-PAb Conjugate-Based Immunochromatographic Assay for Detection of Abrin-a. Monoclonal Antibodies Immunodiagn. Immunother 2015, 34 (5), 341–345.

(13). Garber EA; Walker JL; O'Brien TW Detection of abrin in food using enzyme-linked immunosorbent assay and electrochemiluminescence technologies. J. Food Prot 2008, 71 (9), 1868–1874. [PubMed: 18810871]

(14). Simon S; Worbs S; Avondet MA; Tracz DM; Dano J; Schmidt L; Volland H; Dorner BG; Corbett CR Recommended Immunological Assays to Screen for Ricin-Containing Samples. Toxins 2015, 7 (12), 4967–4986. [PubMed: 26703725]

(15). He X; Patfield S; Cheng LW; Stanker LH; Rasooly R; McKeon TA; Zhang Y; Brandon DL Detection of Abrin Holotoxin Using Novel Monoclonal Antibodies. Toxins 2017, 9 (12), 386. [PubMed: 29182545]

(16). Zhou Y; Tian XL; Li YS; Pan FG; Zhang YY; Zhang JH; Wang XR; Ren HL; Lu SY; Li ZH; et al. Development of a monoclonal antibody-based sandwich-type enzyme-linked immunosorbent assay (ELISA) for detection of abrin in food samples. Food Chem 2012, 135 (4), 2661–2665. [PubMed: 22980855]

(17). Liu Y; Zhan L; Qin Z; Sackrison J; Bischof JC Ultrasensitive and Highly Specific Lateral Flow Assays for Point-of-Care Diagnosis. ACS Nano 2021, 15 (3), 3593–3611. [PubMed: 33607867]

(18). Ramage JG; Prentice KW; Morse SA; Carter AJ; Datta S; Drumgoole R; Gargis SR; Griffin-Thomas L; Hastings R; Masri HP; et al. Comprehensive laboratory evaluation of a specific lateral flow assay for the presumptive identification of abrin in suspicious white powders and environmental samples. Biosecur. Bioterrorism Biodefense Strategy, Pract. Sci 2014, 12 (1), 49–62.

(19). Kalb SR; Schieltz DM; Becher F; Astot C; Fredriksson S; Barr JR Recommended Mass Spectrometry-Based Strategies to Identify Ricin-Containing Samples. Toxins 2015, 7 (12), 4881–4894. [PubMed: 26610568]

(20). Worbs S; Skiba M; Söderström M; Rapinoja ML; Zeleny R; Russmann H; Schimmel H; Vanninen P; Fredriksson S; Dorner BG Characterization of Ricin and R. communis Agglutinin Reference Materials. Toxins 2015, 7 (12), 4906–4934. [PubMed: 26703723]

(21). Luo L; Yang J; Li Z; Xu H; Guo L; Wang L; Wang Y; Luo L; Wang J; Zhang P; et al. Label-free differentiation and quantification of ricin, abrin from their agglutinin biotoxins by surface plasmon resonance. Talanta 2022, 238 (Pt 1), 122860. [PubMed: 34857316]

(22). Worbs S; Kampa B; Skiba M; Hansbauer E-M; Stern D; Volland H; Becher F; Simon S; Dorner MB; Dorner BG Differentiation, Quantification and Identification of Abrin and Abrus precatorius Agglutinin. Toxins 2021, 13 (4), 284. [PubMed: 33919561]

(23). Pauly D; Kirchner S; Stoermann B; Schreiber T; Kaulfuss S; Schade R; Zbinden R; Avondet M-A; Dorner MB; Dorner BG Simultaneous quantification of five bacterial and plant toxins from complex matrices using a multiplexed fluorescent magnetic suspension assay. Analyst 2009, 134 (10), 2028–2039. [PubMed: 19768210]

(24). Ji B; Kenaan A; Gao S; Cheng J; Cui D; Yang H; Wang J; Song J Label-free detection of biotoxins via a photo-induced force infrared spectrum at the single-molecular level. Analyst 2019, 144 (20), 6108–6117. [PubMed: 31532409]

(25). Fredriksson S; Artursson E; Bergström T; Östin A; Nilsson C; Åstot C Identification of RIP-II toxins by affinity enrichment, enzymatic digestion and LC-MS. Anal. Chem 2015, 87 (2), 967–974. [PubMed: 25496503]

(26). Rasooly R; Do P; Hernlem B CCD Based Detector for Detection of Abrin Toxin Activity. Toxins 2020, 12 (2), 120. [PubMed: 32075080]

(27). Makdasi E; Laskar O; Milrot E; Schuster O; Shmaya S; Yitzhaki S Whole-Cell Multiparameter Assay for Ricin and Abrin Activity-Based Digital Holographic Microscopy. Toxins 2019, 11 (3), 174. [PubMed: 30909438]

(28). Kalb SR; Barr JR Mass spectrometric detection of ricin and its activity in food and clinical samples. Anal. Chem 2009, 81 (6), 2037–2042. [PubMed: 19228034]

(29). Wang D; Baudys J; Barr JR; Kalb SR Improved Sensitivity for the Qualitative and Quantitative Analysis of Active Ricin by MALDI-TOF Mass Spectrometry. Anal. Chem 2016, 88 (13), 6867–6872. [PubMed: 27264550]

(30). Becher F; Duriez E; Volland H; Tabet JC; Ezan E Detection of functional ricin by immunoaffinity and liquid chromatography-tandem mass spectrometry. Anal. Chem 2007, 79 (2), 659–665. [PubMed: 17222034]

(31). Hoyt K; Barr JR; Kalb SR Detection of ricin activity and structure by using novel galactose-terminated magnetic bead extraction coupled with mass spectrometric detection. Anal. Biochem 2021, 631, 114364. [PubMed: 34487718]

(32). Frankel AE; Burbage C; Fu T; Tagge E; Chandler J; Willingham MC Ricin Toxin Contains at Least Three Galactose-Binding Sites Located in B Chain Subdomains 1α, 1β, and 2γ. Biochemistry 1996, 35 (47), 14749–14756. [PubMed: 8942636]

(33). Olsnes S; Saltvedt E; Pihl A Isolation and Comparison of Galactose-binding Lectins from Abrus precatorius and Ricinus communis. J. Biol. Chem 1974, 249 (3), 803–810. [PubMed: 4811904]

(34). Kandasamy K; Selvaprakash K; Chen YC Functional magnetic nanoparticle-based affinity probe for MALDI mass spectrometric detection of ricin B. Mikrochim. Acta 2021, 188 (10), 339. [PubMed: 34510288]

(35). Selvaprakash K; Chen YC Detection of ricin by using gold nanoclusters functionalized with chicken egg white proteins as sensing probes. Biosens. Bioelectron 2017, 92, 410–416. [PubMed: 27836610]

(36). Hodge DR; Prentice KW; Ramage JG; Prezioso S; Gauthier C; Swanson T; Hastings R; Basavanna U; Datta S; Sharma SK; et al. Comprehensive Laboratory Evaluation of a Highly Specific Lateral Flow Assay for the Presumptive Identification of Ricin in Suspicious White Powders and Environmental Samples. Biosecur. Bioterrorism Biodefense Strategy, Pract. Sci 2013, 11 (4), 237–250.

(37). Yamashita K; Tachibana Y; Kobata A The structures of the galactose-containing sugar chains of ovalbumin. J. Biol. Chem 1978, 253 (11), 3862–3869. [PubMed: 649611]

(38). Harvey DJ; Wing DR; Küster B; Wilson IBH Composition of N-linked carbohydrates from ovalbumin and co-purified glycoproteins. J. Am. Soc. Mass Spectrom 2000, 11 (6), 564–571. [PubMed: 10833030]

(39). Wu AM; Wu JH; Herp A; Chow LP; Lin JY Carbohydrate specificity of a toxic lectin, abrin A, from the seeds of Abrus precatorius (jequirity bean). Life Sci 2001, 69 (17), 2027–2038. [PubMed: 11589518]

(40). Wilson DS; Keefe AD; Szostak JW The use of mRNA display to select high-affinity protein-binding peptides. Proc. Natl. Acad. Sci. U.S.A 2001, 98 (7), 3750–3755. [PubMed: 11274392]

(41). Bean BP Nitrendipine block of cardiac calcium channels: high-affinity binding to the inactivated state. Proc. Natl. Acad. Sci. U.S.A 1984, 81 (20), 6388–6392. [PubMed: 6093100]

(42). Schrot J; Weng A; Melzig MF Ribosome-Inactivating and Related Proteins. Toxins 2015, 7 (5), 1556–1615. [PubMed: 26008228]

(43). Wu ZL; Huang X; Burton AJ; Swift KAD Probing sialoglycans on fetal bovine fetuin with azido-sugars using glycosyltransferases. Glycobiology 2015, 26 (4), 329–334. [PubMed: 26589574]

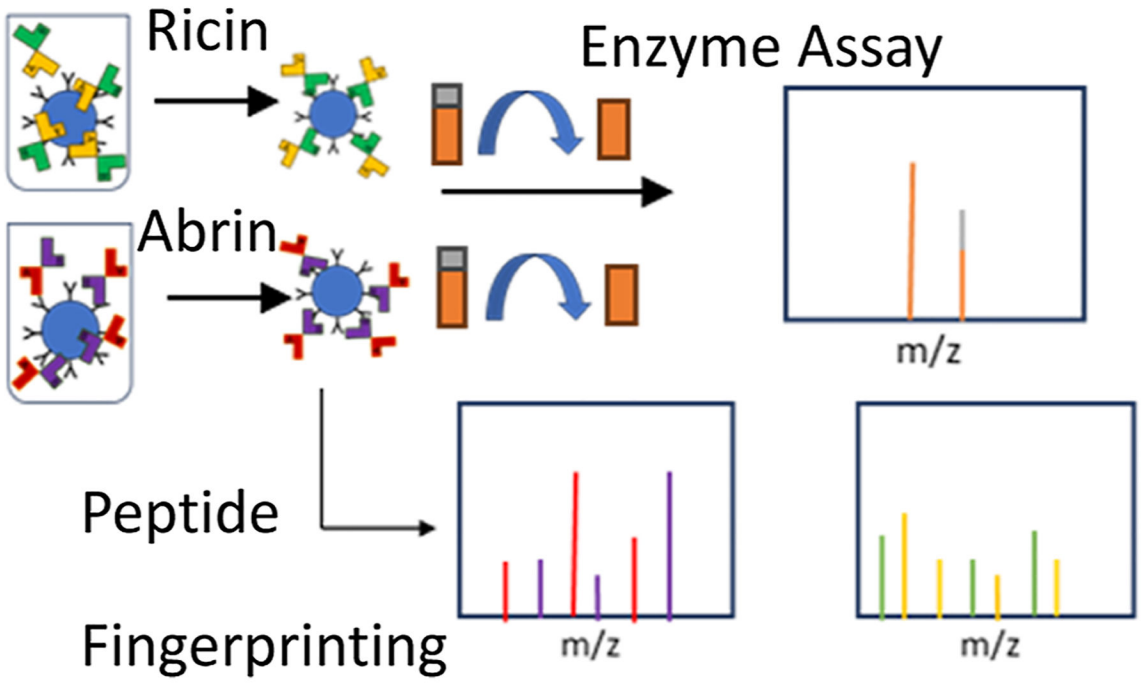

Figure 1.
Schematic of the analytical workflow which includes an enzyme activity assay to mimic the biological activity of ricin and abrin and peptide fingerprinting to differentiate these toxins.

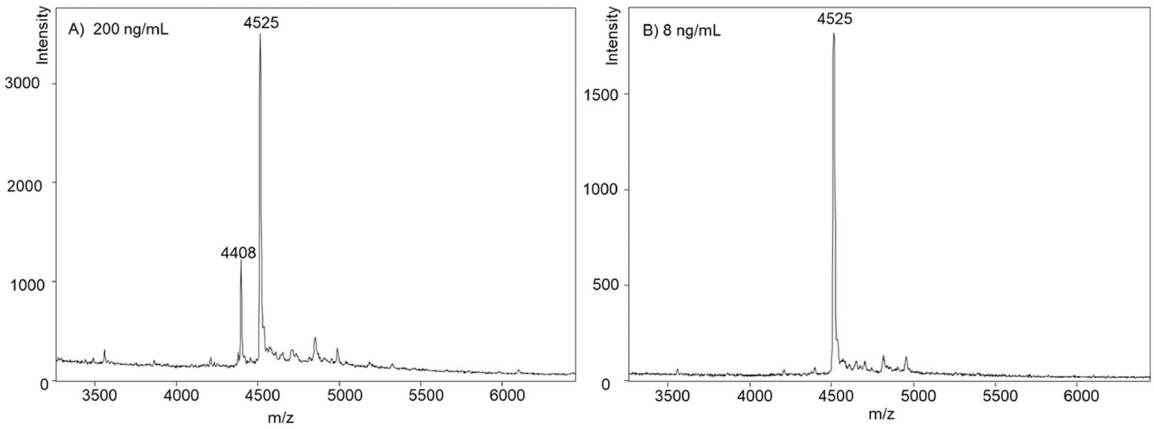

Figure 2.

Mass spectra depicting the RNA substrate with (A) 200 ng/mL of abrin and (B) 8 ng/mL of abrin. Abrin was extracted with 4-APLP beads. The intact RNA substrate can be observed at *m*/*z* 4525 and the depurinated substrate can be observed at *m*/*z* 4408.

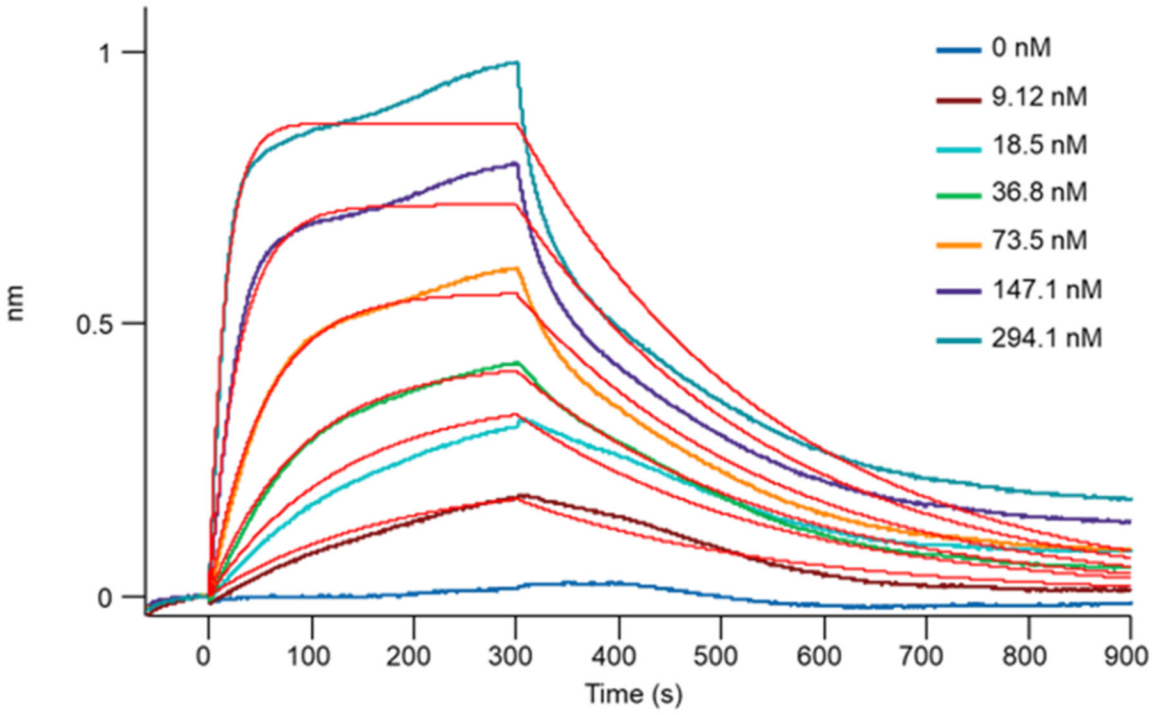

Figure 3.
Binding kinetics of ricin B-chain to asialofetuin.

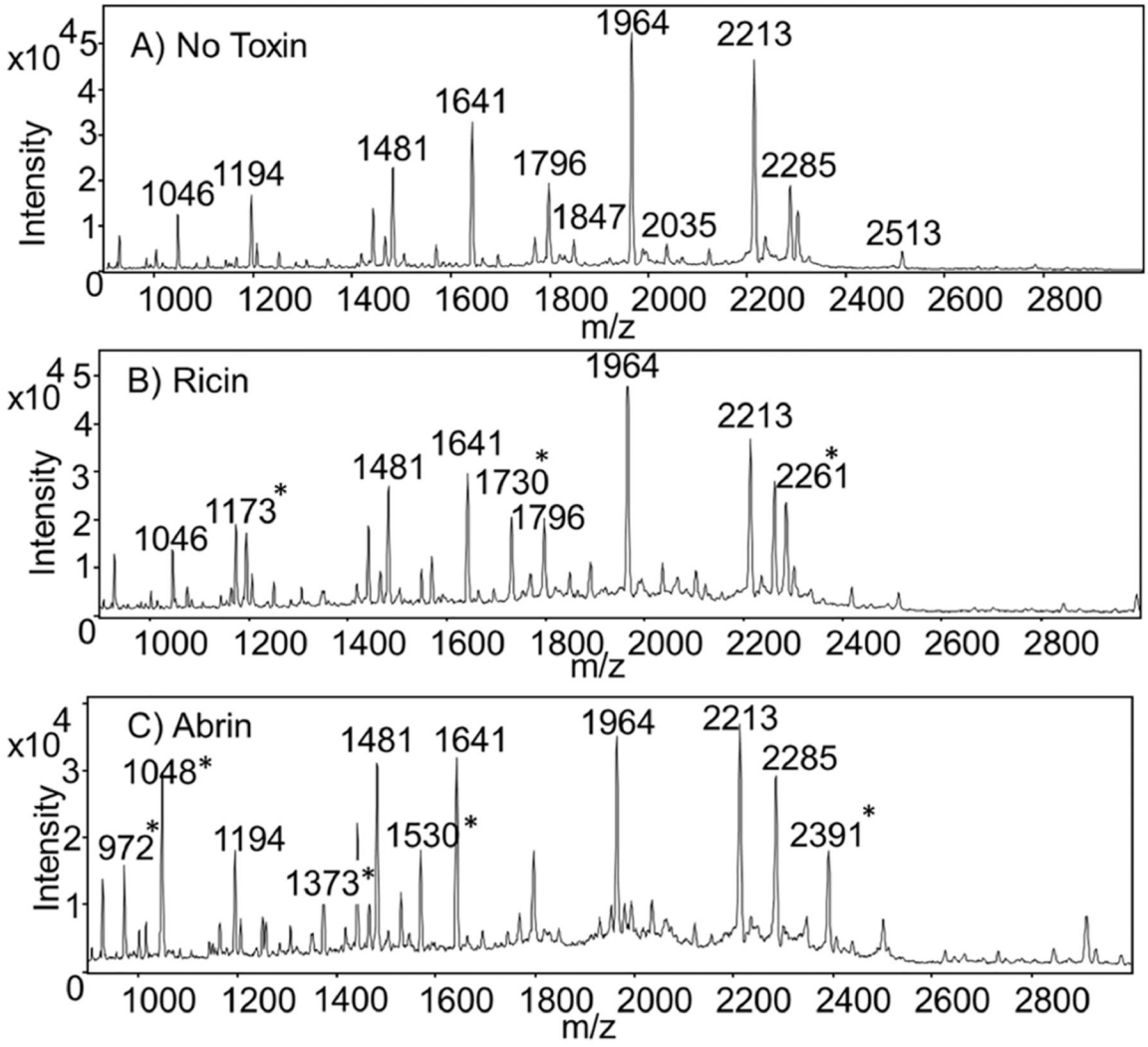

Figure 4.

Mass spectra of tryptic digests of (A) no toxin, (B) ricin, and (C) abrin, with toxin fragments indicated by asterisk.

Table 1.

Ligand and Bead Combinations Tested for Extracting Abrin[a]

Ligand	Bead			
	Amine terminated	Aldehyde terminated	Long arm aldehyde terminated	Dynabeads streptavadin
D-(+) Glucosamine hydrochloride	X	X	X	
D(+)Galactoseamine Hydrochloride	X	X	X	
2-Aminoethyl β-N-Acetylglucoseamine	X	X		
2-Aminoethyl α-Galactopyranoside	X	X		

Ligand	Bead			
	Amine terminated	Aldehyde terminated	Long arm aldehyde terminated	Dynabeads streptavadin
2-Aminoethyl β-Glucopyranoside	✗	✗		
2-Aminoethyl β-Lactopyranoside	✗	✗		
4-Aminoethyl-β-D-Lactopyranoside (4-APLP)	✓	✗		
Ovalbumin				✗

Ligand	Bead			
	Amine terminated	Aldehyde terminated	Long arm aldehyde terminated	Dynabeads streptavadin
Fetuin from fetal calf serum				✓
Asialofetuin from fetal calf serum				✓
α1-acid glycoprotein				✓

[a]The red "x" indicates the inability to extract abrin at detectable levels; the green checkmark indicates the ability to extract abrin at detectable levels.

Table 2.

Results of LOD Studies for Abrin

Abrin				
Trial	**Blank**	**2 ng**	**4 ng**	**6 ng**
1	0	0.09	0.11	0.08
2	0.03	0	0.1	0.12
3	0.02	0.13	0.13	0.06
4	0	0.13	0.18	0.14
5	0	0.1	0.07	0.12
6	0	0.11	0.11	0.08
7	0.04	0.11	0.16	0.06
8	0.03	0.09	0.09	0.12
9	0	0.11	0.1	0.12
10	0	0	0.08	0.1
11	0	0	0.09	0.09
12	0	0.05	0.13	0.1
13	0	0	0.1	0.12
14	0	0.05	0.14	0.15
15	0	0.06	0.16	0.08
16	0.03	0	0.1	0.1
17	0	0	0.16	0.11
18	0	0	0.09	0.12
19	0.05	0	0.1	0.1
20	0.03	0	0.09	0.09
Average blank	0.01			
3x average blank	0.03			
Total positive		**55%**	**100%**	**100%**

Table 3.

Results of LOD Studies for Ricin

Ricin				
Trial	**Blank**	**50 pg**	**75 pg**	**100 pg**
1	0	0.08	0.09	0.12
2	0	0	0.09	0.14
3	0	0.09	0.09	0.1
4	0	0.21	0.11	0.15
5	0.03	0.09	0.16	0.17
6	0	0	0.15	0.19
7	0	0	0.12	0.11
8	0.03	0.08	0.1	0.14
9	0	0.1	0.1	0.21
10	0.02	0.1	0.13	0.15
11	0	0.08	0.14	0.14
12	0.02	0.12	0.15	0.26
13	0.01	0.08	0.14	0.18
14	0.02	0.07	0.11	0.18
15	0	0.07	0.1	0.12
16	0.01	0.09	0.13	0.14
17	0	0.08	0.13	0.16
18	0	0.11	0.17	0.22
19	0	0.11	0.09	0.12
20	0	0	0.1	0.18
Average blank	0.01			
3x average blank	0.03			
Total positive		**80%**	**100%**	**100%**

Chem Res Toxicol. Author manuscript; available in PMC 2024 July 21.

Table 4.

Tryptic Fragments Used to Differentiate between Ricin and Abrin

R. Communis		A. Precatorius	
m/z	**squence**	***m/z***	**squence**
878	IRYNRR	972	ISLGLEALR
1173	FQYIEGEMR	1048	AGSESFFFR
1730	SAPDPSVITLENSWGR	1373	LTGGLIYGIPVLR
1888	RSAPDPSVITLENSWGR	1530	TLIVIIQMVAEAAR
2260	LSTAIQESNQGAFASPIQLQR	2391	AAFQPDPSMLSLENTWESPLSR
3310	AGNSAYFFHPDNQEDAEAITHLTDVQNR		

Table 5.

Results of Near Neighbor Study Related to Abrin and Ricin Detection

	Activity		Structure	
	Blank	**Sample**	**Blank**	**Sample**
V. album	Negative	Negative		
S. ebulus	Negative	Negative		
S. occidentalis	Negative	Negative		
C. camphora	Negative	Positive	Negative	Negative
I. hollandica	Negative	Negative		
S. nigra	Negative	Positive	Negative	Negative
Shiga Toxin	Negative	Negative		

Chem Res Toxicol. Author manuscript; available in PMC 2024 July 21.

Table 6.

Results of White Powder Study Related to Abrin and Ricin Detection Coupled with the Addition of Lactase Prior to Toxin Extraction

	Activity		Structure	
	Blank	**Sample**	**Blank**	**Sample**
Baby Powder	Negative	Positive	Negative	Positive
Baking Mix	Negative	Positive	Negative	Positive
Baking Powder	Negative	Positive	Negative	Positive
Baking Soda	Negative	Positive	Negative	Positive
Chalk Dust	Negative	Positive	Negative	Positive
Coffee Creamer	Negative	Positive	Negative	Positive
Corn Starch	Negative	Positive	Negative	Positive
Decongestant	Negative	Positive	Negative	Positive
Dry Milk	Negative	Positive	Negative	Positive
Epsom Salt	Negative	Positive	Negative	Positive
Eye Shadow	Negative	Positive	Negative	Positive
Flour	Negative	Positive	Negative	Positive
Glutamine	Negative	Positive	Negative	Positive
Parmesan Cheese	Negative	Positive	Negative	Positive
Powdered Sugar	Negative	Positive	Negative	Positive